



---

## Crucial CD8<sup>+</sup> T-lymphocyte cytotoxic role in amphotericin B nanospheres efficacy against experimental visceral leishmaniasis

---

Sofia A. Costa Lima<sup>a,□,1</sup>, Ricardo Silvestre<sup>a</sup>, Daniela Barros<sup>a</sup>, Joana Cunha<sup>a,b</sup>, Maria Teresa Baltazar<sup>c,d,e</sup>, Ricardo Jorge Dinis Oliveira<sup>c,d,e,f</sup>, Anabela Cordeiro-da-Silva<sup>a,g</sup>

<sup>a</sup> IBMC-INEB, Infection and Immunology Unit, Parasite Disease Group, University of Porto, Portugal;

<sup>b</sup> Instituto de Ciências Biomédicas Abel Salazar e Faculdade de Medicina, Universidade do Porto, Portugal;

<sup>c</sup> IINFACTS - Institute of Research and Advanced Training in Health Sciences and Technologies, Department of Sciences, Advanced Institute of Health Sciences-North (ISCS-N), CESPU, CRL, Gandra, Portugal;

<sup>d</sup> Department of Legal Medicine and Forensic Sciences, Faculty of Medicine, University of Porto, Porto, Portugal;

<sup>e</sup> REQUIMTE, Laboratory of Toxicology, Department of Biological Sciences, Faculty of Pharmacy, University of Porto, Porto, Portugal

<sup>f</sup> Forensic Sciences Center (CENCIFOR), Portugal;

<sup>g</sup> Department of Biological Sciences, Faculty of Pharmacy, University of Porto, Portugal.

E-mail address: [slima@ff.up.pt](mailto:slima@ff.up.pt) (S.A. Costa Lima).

**Keywords:** Amphotericin B; Poly(D,L-lactide-co-glycolide) nanospheres; Visceral leishmaniasis; Immune-modulation; CD8<sup>+</sup> T lymphocytes

Originally published at *Nanomedicine: Nanotechnology, Biology and Medicine*, 2014, 10(5):1021-30, doi: 10.1016/j.nano.2013.12.013, Elsevier

INSTITUTO  
DE INVESTIGAÇÃO  
E INOVAÇÃO  
EM SAÚDE  
UNIVERSIDADE  
DO PORTO

Rua Alfredo Allen, 208  
4200-135 Porto  
Portugal  
+351 220 408 800  
info@i3s.up.pt  
[www.i3s.up.pt](http://www.i3s.up.pt)

Version: Postprint (identical content as published paper) This is a self-archived document from i3S – Instituto de Investigação e Inovação em Saúde in the University of Porto Open Repository For Open Access to more of our publications, please visit <http://repositorio-aberto.up.pt/>

## ABSTRACT

This work aims to develop poly(d,l-lactide-co-glycolide) (PLGA)-nanospheres containing amphotericin B (AmB) with suitable physicochemical properties and anti-parasitic activity for visceral leishmaniasis (VL) therapy. When compared with unloaded-PLGA-nanospheres, the AmB-loaded PLGA-nanospheres displayed an increased particle size without affecting the polydispersity and its negative surface charge. AmB stability in the PLGA-nanospheres was > 90% over 60-days at 30 °C. The AmB-PLGA-nanospheres demonstrated significant *in vitro* and *in vivo* efficacy and preferential accumulation in the visceral organs. In addition, an immune-modulatory effect was observed in mice treated with AmB-PLGA-nanospheres, correlating with improved treatment efficacy. The *in vitro* cytotoxic response of the T-lymphocytes revealed that AmB-PLGA-nanospheres efficacy against VL infection was strictly due to the action of CD8<sup>+</sup> but not CD4<sup>+</sup>-T lymphocytes. Overall, we demonstrate a crucial role for CD8<sup>+</sup> cytotoxic T lymphocytes in the efficacy of AmB-PLGA nanospheres, which could represent a potent and affordable alternative for VL therapy.

## FROM THE CLINICAL EDITOR

This study demonstrates a crucial role for CD8<sup>+</sup> T lymphocytes in eliminating visceral leishmaniasis in a murine model by enhancing the cytotoxic efficacy of CD8<sup>+</sup> T-cells via amphotericin-B-PLGA nanospheres, paving a way to a unique, potentially more potent and cost-effective therapeutic strategy.

## INTRODUCTION

Amphotericin B (AmB) is a polyene antibiotic, approved by the FDA, which is commonly used to treat invasive fungal infections and as second-line drug in the treatment of visceral leishmaniasis (VL). AmB is produced by *Streptomyces* sp. and has low solubility at physiological pH (< 0.1 mg/mL), which restrains the development of pharmaceutical formulations for oral and parenteral administrations (1, 2). The connection between its physico-chemical properties, pharmacokinetics and pharmacodynamics remains uncertain (3-5). It has a high VL curative rate but requires prolonged period of treatment and hospitalization, leading to renal toxicity, among other severe adverse reactions. Indeed, the extensive association of AmB with low density lipoproteins (LDL) and the internalization of the AmB-LDL complex by kidney cells rich in high affinity LDL receptors responsible for the nephrotoxicity is well known (4, 6).

Leishmaniasis is a protozoan disease spread in nearly one hundred countries worldwide and is listed as the second major human neglected tropical disease in terms of mortality and morbidity with 350 million people living at risk, and a prevalence of 2 million cases a year, of which 0.5 million cases are of VL, a potentially fatal disease if left untreated. However, the treatment options are limited and unsatisfactory since most available drugs require parenteral

administration and present serious toxicity with the occurrence of resistant strains contributing to hamper their success.

Drug delivery systems (DDSs) are a well-established approach to improve the therapeutic efficiency of drugs with concomitant reduction of drug toxicity. Several AmB lipid formulations (AmBisome®, Amphocil® and Abelcet®) and other DDSs have been developed in the past few years, but only the liposomal formulation AmBisome® has become a standard treatment for VL (6, 7). Recently, a single-course therapy of 10 mg/kg has been shown to cure 95% of VL patients in India (8). AmBisome® is significantly less toxic than the conventional AmB colloidal dispersion with sodium deoxycholate (Fungizone®) developed in 1958 (9, 10) since the former alters the pharmacokinetics, distribution and excretion profiles of AmB by decreasing free AmB concentrations in plasma as a result of encapsulation of the drug in liposomes (11, 12). Still, there are limitations for AmBisome® treatment among which the high cost and temperature stability (recommended 25 °C for unopened vials of lyophilized material and 2-8 °C/24 h for reconstituted vials, accordingly to the manufacturer) comprise the major drawbacks.<sup>5</sup> Moreover, AmB repeated administrations result in its accumulation due to slow elimination from the body, ultimately leading to nephrotoxicity (13). In view of all these facts, the search for a safer, more potent and especially more cost-effective AmB delivery system still remains. Recently, new DDSs for AmB have been described but some issues related with efficacy, toxicity and stability still remain (14-19).

The present work aims to produce a nanospheres-based delivery system for AmB in an attempt to develop a cost-effective formulation with reduced toxicity, increased temperature stability and retaining its efficiency to VL treatment. To overcome AmB's drawbacks, we considered that a low-dose therapeutic system for AmB is desirable, aiming specifically to reduce the side-effects while maintaining its anti-parasitic efficacy. In order to develop such a delivery system for AmB, polymeric nanospheres (NS) based on Poly(D,L-lactide-co-glycolide) (PLGA) were selected due to their sustained-release characteristics, easy scale up, simple transformation, small particle size, biodegradability and biocompatibility properties (20). These are crucial properties to ensure an intracellular delivery and sustained release of drugs at a therapeutically relevant level (21). Here, we report the preparation and physicochemical characterization of the AmB-PLGA-NS followed by the *in vitro* and *in vivo* evaluation of the anti-leishmanial activity in comparison to free AmB or its commercially available lipid formulations. In parallel, we evaluated the *in vivo* AmB's distribution and drug-induced toxicity in several organs and unravel the probable interaction of this novel nano-formulation with the immune response.

## METHODS

Detailed descriptions of the materials and methods can be found in the Supplementary Material

**Ethics statement.** All procedures involving animals were approved by and performed in accordance with the Portuguese National Authority for Animal Health license (0042/000/2012) and, the requirements and regulations laid down by the ethical review of IBMC-INEB Animal Ethics Committee.

**Preparation and physical characterization of AmB-loaded PLGA nanospheres.** Drug loaded PLGA-NS were prepared based on the nanoprecipitation method (22). The mean particle size, size distribution and zeta potential ( $\zeta$ -potential) of the nanoformulations were determined with a Zetasizer Nano ZS detector (Malvern Instruments, Worcestershire, UK). The morphology of NS was observed by transmission electronic microscopy (TEM) (TEM Jeol JEM-1400, Tokyo, Japan). AmB loading on the PLGA-NS was determined directly by measuring the amount of drug entrapped in the NS by an Ultra Performance Liquid Chromatography (UPLC) method described in the Supplementary Material (Table S1).

**Parasites, cell culture, infection of mice and treatment schedules.** For experimental infections, BALB/c mice (6-8 weeks old) were injected intraperitoneally (i.p.) with  $10^8$  stationary phase promastigotes. Infected mice (6 mice/group) received i.v. injection of a single-shot treatment of drug-free PLGA-NS (1.5 mg/mouse), AmBisome® (1 mg/kg), and a single or three consecutive daily doses of AmB-PLGA-NS (1 mg/kg AmB associated with 1.5 mg of PLGA-NS) after 14-days of infection.

**In vivo AmB distribution.** The analysis of AmB in tissues samples was based on a previously described analytical method (23). Homogenized tissues were used for the UPLC analysis and the limit of AmB quantification was 20 ng/mL.

**T cell proliferation assay.** T cell proliferation assay was performed with splenocytes from different experimental groups of treated and untreated mice isolated by mechanical disruption. After 96 h the proliferation of splenic lymphocytes labeled with carboxyfluorescein succinimidyl ester was evaluated by flow cytometry, and T-cell populations identified with APC-conjugated anti-mouse CD4 and PB-conjugated anti-mouse CD8.

**Analysis of cytokines and total nitrites production.** Secreted cytokines were quantified in the splenocytes culture supernatants of differently treated infected mice by ELISA as recommended by the manufacturer (BioLegend, San Diego CA, USA). The total nitrite oxide (NO) content was quantified in supernatants of 72 h-culture of splenocytes recovered from the different treatment animal groups stimulated, or not, with soluble *Leishmania* antigens (SLA) using the Griess method (24).

**In vitro cell-mediated cytotoxicity assays.** The *in vitro* cytotoxicity assay was accomplished using a LIVE/DEAD cell-mediated cytotoxicity kit (Molecular Probes, Invitrogen Life Technologies, Alfragide, Portugal) according to the manufacturer's protocol.

## RESULTS

**Physicochemical characterization of nanospheres: size, zeta potential, morphology, drug content, storage stability and in vitro release.** AmB was encapsulated into PLGA-NS by nanoprecipitation,<sup>22</sup> following an optimization step described in Supplementary Material (Table S2). The physicochemical properties of the optimized NS such as particle size, polydispersity (PDI),  $\xi$ -potential and drug encapsulation efficiency (EE) were studied and are summarized in Table 1.

The nanoformulations displayed mean diameter of  $187.3 \pm 1.3$  to  $221.5 \pm 6.6$  nm for empty and AmB-PLGA-NS, respectively, with low PDI. Loading of the PLGA-NS with AmB led to a statistically significant increase on the size ( $P < 0.05$ ) without disturbing the PDI or the

surface charge as shown by constant  $\zeta$ -potential values around  $-18$  mV. TEM photographs revealed that empty (Figure 1, A) and AmB-PLGA-NS (Figure 1, B) were found to be homogeneous and spherically shaped. Moreover, the AmB-PLGA-NS could be obtained in a reproducible and industrial-sized production within a short period of time (6 h). The encapsulation efficiency was determined by UPLC analysis of AmB-loaded nanoformulations. The AmB loading was calculated to be about  $130 \mu\text{g}/\text{mg}$  of PLGA, which represented an EE of 65%.

The influence of pH on the AmB release profile from the PLGA-NS for 10-days is shown on Figure 1, C. For both physiologic and acidic pH conditions the NS displayed a biphasic pattern characterized by a burst release of AmB that lasted approximately 6 h, followed by a continuous release of the drug for at least 10-days. Yet, the effect observed during the first phase of release was much more drastic at acidic than at physiologic pH ( $P < 0.05$ ).

The AmB-PLGA and unloaded PLGA-NS did not show any signs of aggregation during the purification steps and remained stable upon storage at  $4^\circ\text{C}$  for at least 60-days, as no significant changes were observed on their particle size, PDI and  $\zeta$ -potential (Figure 1, D-E). With the increase of the storage period the nanoformulations were found slightly less negative than the freshly prepared nanoformulations ( $P < 0.05$ ) (Figure 1, D) with higher tendency to aggregate (PDI  $> 0.1$ ) and a non-significant size increase (Figure 1, E). No modification was found on the AmB content when the PLGA-NS were stored at  $4^\circ\text{C}$  up to 60-days (data not shown).

To evaluate the *in vitro* stability of AmB-PLGA-NS under sub-tropical and tropical temperatures, the nanoformulations were incubated at  $30$  and  $42^\circ\text{C}$ . Regarding the drug content, the temperature did not affect the stability of AmB in PLGA-NS, exceeding  $94.38\% \pm 3.56\%$  (Figure S1D, light grey) and  $86.12\% \pm 4.28\%$  (Figure S1D, dark grey) of its initial concentration after 30-days at  $30^\circ\text{C}$  or  $42^\circ\text{C}$ , respectively. Nevertheless, this decrease on the AmB content inside the PLGA-NS did not affect its efficacy. Indeed, the anti-leishmanial activity of AmB-PLGA-NS stored at  $30^\circ\text{C}$  for 60-days exhibited an  $\text{IC}_{50}$  value of  $0.16 \pm 0.03 \mu\text{g}/\text{mL}$  against intracellular *L. infantum* amastigotes in THP1 differentiated macrophages, which is remarkably similar to the one observed with freshly prepared NS ( $0.13 \pm 0.02 \mu\text{g}/\text{mL}$ ,  $p > 0.05$ ).

***In vivo* efficacy of the AmB-PLGA nanospheres.** AmB-PLGA-NS led to a marked *in vitro* anti-leishmanial outcome (Figure S2, Table S3) hence the efficacy of the AmB-PLGA-NS was assessed in a VL susceptible murine model by a single- or a three-daily dose treatment at  $1 \text{ mg}/\text{kg}$ . In all treated groups a significant reduction ( $P < 0.001$ ) of the parasite load was found on the splenic and hepatic tissues (Figure 2, A and B). When given in a single-dose or 3-daily doses at  $1 \text{ mg}/\text{kg}$ , AmB-PLGA-NS promoted a reduction of  $98.6\% \pm 1.4\%$  and  $99.3\% \pm 0.5\%$ , respectively, in the splenic parasites corresponding to approximately 100-fold decrease, as compared to the vehicle control. Concerning the liver, a less effective outcome was observed, with  $90.6\% \pm 0.7\%$  and  $98.7\% \pm 0.8\%$  parasite reduction for AmB-PLGA-NS given in single or 3-daily doses, respectively, related to the vehicle control. Importantly, the AmB-PLGA-NS led to a more pronounced reduction on the splenic parasites when compared with AmBisome® irrespective of the number of doses given ( $P < 0.05$ ) (Figure 2, A). In the liver, a 3-consecutive daily dose was as effective as AmBisome® in reducing the parasite burden (Figure 2, B).

***In vivo* AmB distribution.** In order to clarify the high splenic efficacy of AmB-PLGA-NS we were interested in understanding the distribution pattern of AmB when given as Fungizone®

(0.8 mg/kg), AmBisome® (1 mg/kg) and PLGA NS (1 mg/kg) by i.v. to infected animals. Fungizone® was chosen for comparison as another amphotericin B formulation clinically used. The results of tissue distribution of AmB 2 h following i.v. administration of the three formulations are summarized in Table 2.

Following i.v. administration of PLGA-NS and AmBisome®, AmB accumulates mainly in the spleen and liver, in comparison to other tissues (kidney, lung and heart). Furthermore, an impressive amount of AmB from the PLGA-NS is focused on the spleen, being approximately 2-fold less present in the liver. In opposition, AmB delivered by AmBisome® accumulates twice more in the liver than in the spleen. Even so, the overall concentrations in these two *Leishmania*-target organs are not significantly different for those two AmB formulations.

**Toxicological studies.** The safety of a new VL treatment is as fundamental as its efficacy. By assessing the oxidative stress it is possible to ascertain tissue toxicity elicited by the administration of the AmB treatments (25). Therefore, we evaluated biomarkers of oxidative stress in the liver and spleen, namely reduced (GSH) and oxidized glutathione (GSSG).

The measurement of the ratio of reduced GSH to GSSG in the liver showed a statistical significant decrease ( $P < 0.01$ ) for PLGA-NS-, single- and 3-consecutive doses-AmB-PLGA-NS, and AmBisome®-treated groups when compared with the untreated group (Figure 3, A). Similarly, in the spleen (Figure 3, B) a statistical decrease ( $P < 0.05$ ) for PLGA-AmB-treated group was observed. The extent of drug-induced tissue toxicity by ROS was further determined by means of lipid peroxidation and myeloperoxidase activities in the liver and spleen, but no statistically significant differences were observed within all the experimental groups in the tissues analyzed (Figure S3).

**AmB-PLGA nanospheres positively interact with the immune system.** Further experiments were performed to evaluate if AmB-PLGA-NS induce a protective modulation of adaptive immunity besides the anti-leishmanial activity in VL mice model.

Splenocytes from AmB-PLGA-NS treated animals showed enhanced CD4<sup>+</sup> and CD8<sup>+</sup>-T cell proliferation in response to SLA ( $P < 0.001$ ), while empty NS and AmBisome® treatment had little or no effect on lymphocytes proliferation (Figure 4, A). Even though the development of T cell specific proliferation was observed with a single-dose of AmB-PLGA-NS, the effect was more pronounced with the 3-consecutive daily administrations (Figure 4, A). The development of a T-cell specific response did not result from a quantitative modification of the spleen cellular populations (Figure S4) or to significant changes on their activation status (Figure S5). Instead, we detected a significant increase on the number of effector memory CD8<sup>+</sup>-T cells (Figure 4, B), and CD4<sup>+</sup>-T cells to a lower extent (~ 4%, Figure S6), after treatment with AmB-PLGA-NS. Indeed, the analysis of the CD8<sup>+</sup>-T cell phenotype obtained from AmB-PLGA-NS treated mice revealed a predominant effector memory subset (CD44<sup>+</sup>CD62L<sup>low</sup>) as compared to CD8<sup>+</sup>-T cells from controls (Figure 4, B). These qualitative changes in the lymphocytes subpopulations led us to investigate their function in terms of cytokine profile developed during AmB-PLGA-NS treatment. We detected a 1.5- ( $P < 0.05$ ) and 2-fold ( $P < 0.001$ ) increase in the frequencies of IFN $\gamma$ <sup>+</sup> CD4<sup>+</sup>-T cells and 2.6 ( $P < 0.01$ ) and 5.1-fold ( $P < 0.001$ ) enhancement of IFN $\gamma$ <sup>+</sup>-CD8<sup>+</sup> T cells exclusively for the groups that received a single-dose and a 3-consecutive daily doses of AmB-PLGA-NS, respectively (Figure 4, C). Although AmBisome® has proved to elicit similar reductions on parasite burden, we did not detect any significant production of IFN- $\gamma$  in both splenic CD4<sup>+</sup> or CD8<sup>+</sup>-T cells. In all the treated groups (PLGA, AmB-PLGA-NS and AmBisome®), IL-10<sup>+</sup> producing CD4<sup>+</sup> and CD8<sup>+</sup>-T cell

populations did not change with respect to untreated controls (Figure S7A, B). Moreover, the IFN- $\gamma$ <sup>+</sup> producing CD4<sup>+</sup>-T cells developed in AmB-PLGA-NS treated mice failed to produce IL-10 (data not shown). The cytokine quantification of splenocytes supernatants re-stimulated with SLA confirmed these findings. AmB-PLGA-NS treated mice exhibited IL-12 and IFN- $\gamma$  levels significantly higher ( $P < 0.001$ ) in comparison with untreated, AmBisome® or empty PLGA-NS treated infected animals (Figure 4, D). Indeed, IL-12 was ~ 2- and 3-fold higher in single and 3-consecutive daily doses, respectively, which may account for the increase of IFN- $\gamma$  levels in 8 and 11.5-fold in the animals that received single and 3-doses, respectively, of AmB-PLGA-NS. In opposition, IL-10 secretion was found to be restrained in both AmB-PLGA-NS or AmBisome® treated infected animals (Figure 4, D). This cytokinic microenvironment ultimately resulted in an increase of NO production (Figure 4, E). The AmB-PLGA-NS treated animals had a 5- and 6-fold increase in nitrite production, for single and 3-consecutive daily doses, respectively in comparison with the infected untreated animals, while AmBisome® treated animals showed a 2-fold increase when compared with infected untreated animals (Figure 4, E).

*Leishmania*-specific cell-mediated response by antigen-specific cytotoxic T lymphocytes or innate cells is a part of the effective immune response developed against the parasite (26). Antigen-specific cytotoxic T lymphocytes or innate cells are responsible for this cytotoxic activity. In this study, our results provided evidence that the immune-stimulatory effect of AmB-PLGA-NS treatment acts by creating an immunological environment unfavorable for parasite survival and growth. Thus, we have investigated if the AmB-PLGA-NS treatment is also able to induce a *Leishmania*-specific cytotoxic response. Splenocytes from all experimental treatment groups were stimulated *ex vivo* with SLA for 7-days, to favor the expansion of *Leishmania*-specific clones. The cytotoxic response of these cells was then evaluated against *L. infantum*-infected macrophages, revealing a dose-dependent lysis of the target cells (infected macrophages) (Figure 4, F). Indeed, splenocytes recovered from AmB-PLGA-NS treated mice were able to elicit a statistically significant ( $P < 0.001$ ) dose dependent lysis of the target cells of 31.5% and 28.2% for a 3-consecutive daily doses and a single-dose, respectively, at 40:1 (effector: target) ratio. In opposition, empty PLGA-NS or AmBisome® treated infected mice showed no specific cytolysis (Figure 4, F). These results demonstrate that AmB-PLGA-NS induced the generation of *Leishmania*-specific effector cytotoxic T cells that act synergistically with the anti-leishmanial activity of AmB in the elimination of infected macrophages. Importantly, this AmB-PLGA-NS formulation induced a strong adaptive immune response in addition to the anti-parasitic effect, which is absent upon treatment with the AmBisome® formulation.

**Efficacy of AmB-PLGA nanospheres is associated with CD8<sup>+</sup> T cells.** Our results demonstrate that the AmB-PLGA-NS amplified the cellular response to *Leishmania* infection manifested by the development of antigen-specific T lymphocytes with the concomitant secretion of IFN- $\gamma$ . Previous studies have demonstrated that CD4<sup>+</sup> and CD8<sup>+</sup>-T cells play a crucial role in the control of *Leishmania* infection characterized by IFN- $\gamma$  secretion (27, 28). To ascertain the relevant cellular mechanisms responsible for the improved protection induced by the AmB-PLGA-NS, we separately assessed the contributive role of each player (IFN- $\gamma$  and CD4<sup>+</sup>, CD8<sup>+</sup>-T cells). Surprisingly, AmB-PLGA-NS was as effective in reducing the parasite load in spleen and liver of IFN- $\gamma$ <sup>-/-</sup> mice as the wild type control (Figure S8). Since our results demonstrate a *Leishmania*-specific T cell response upon AmB-PLGA-NS treatment (Figure 4, F), we investigated separately the potential role of CD4<sup>+</sup>- and CD8<sup>+</sup>-T cells. To do so, we have depleted each population before AmB-PLGA-NS treatment by injecting *L. infantum* infected BALB/c mice with anti-CD8 or anti-CD4 monoclonal antibody (Figure S9). Remarkably, the treatment with AmB-PLGA-NS failed to control the infection in CD8<sup>+</sup> depleted mice (Figure 5,

A). Mice depleted of CD4<sup>+</sup> cells but maintaining functional CD8<sup>+</sup>-T cells were fully capable to elicit a reduction on the parasite burden after AmB-PLGA-NS treatment (Figure 5, A). In addition, the depletion of CD8<sup>+</sup>-T cells abrogated the cytotoxic activity of AmB-PLGA-NS-pulsed splenocytes against infected host macrophage cells (Figure 5, B) while the depletion of CD4<sup>+</sup>-T cells had little effect. Finally, only CD8<sup>+</sup>-T cells purified from the spleen of AmB-PLGA-NS treated infected mice exhibited similarly a cytotoxic activity upon infected host macrophages (Figure 5, C). These data demonstrate the crucial role for *Leishmania*-specific cytotoxic CD8<sup>+</sup>-T effector cells in the killing of *L. infantum*-infected macrophages in mice that have previously received AmB-PLGA-NS.

## RESULTS

A low cost polymeric system for AmB using PLGA nanospheres was described. Our approach produced a tropically stable and safe DDS with an insight on the splenic cellular immune mechanisms responsible for the efficient response after VL treatment.

When defining a DDS for AmB it is important to consider the hydrophobicity of the compound and the importance of its controlled and sustained release into the surrounding environment. Biodegradable nanoparticles can be produced from natural or synthetic polymers, the latter being advantageous for prolonged release of the encapsulated therapeutic agents that can span for some days to several weeks (29). The polylactides and PLGA are among the most extensively investigated for drug delivery (30). As polyesters in nature, these polymers undergo hydrolysis in the body, forming moieties that are eventually removed from the body by the citric acid cycle. Introduced by Fessi (22) nanoprecipitation is a simple and mild method for the preparation of nanoparticles without the use of any preliminary emulsification. This method presents several advantages, since it does not involve aggressive steps (such as sonication, high temperatures and extended stirring rates), surfactants are not always needed and the organic solvents normally used do not display significant toxicity and, it is highly recommended for hydrophobic drugs (31, 32) Taking all these into consideration, the development of the AmB DDS was primarily based on the PLGA polymer and the nanoprecipitation method. Starting with a small AmB amount the drug was successfully loaded on PLGA-NS with a 65% EE value, which can be related to the nanospheres preparation method but also to the possible electrostatic interaction between capped carboxyl groups of PLGA and the positively charged primary amine group of AmB contributing to such a drug entrapment. Comparable drug EE values above 50% for AmB in PLGA nanoparticles are described in literature with higher initial drug loading values (10% to 30%) (15, 16). The AmB entrapment on the PLGA-NS leads to a statistically significant increase of about 30-nm on the nanospheres size ( $P < 0.05$ ) without affecting the morphology, PDI and  $\zeta$ -potential. It is well established that the stabilizer PVA forms a layer protecting the nanospheres from aggregation and that its residual amount remaining onto the nanospheres is relatively high due to strong attachment to the surface (33).

Assessment of the AmB *in vitro* release revealed pH dependence and since in VL the pathogen resides inside an acidic phagolysosome of macrophages, the AmB *in vitro* release profile suggests retention of the drug inside the NS on the mammalian cell cytoplasm and preferential release at the endosomal-lysosomal acidic pH. Indeed, after 6 h at pH 5.5, 49.99%  $\pm$  2.92% was found to be released from the NS whereas only 18.56%  $\pm$  2.16% of AmB was released from the PLGA-NS under pH 7.4. Afterwards, a similar tendency of slower drug release was maintained for the period of 10-days, revealing 88.40%  $\pm$  3.56% and





60.23%  $\pm$  2.03% AmB released from the PLGA-NS under acidic pH and physiological conditions, respectively.

Based on the accelerated temperature studies set out by the WHO to mimic tropical climate Zone 3 and 4 conditions (34), we analyzed the storage stability of the developed AmB-PLGA-NS at 30 °C and 42 °C in defined time points over a 60-day period. Our nanoformulations improved AmB stability when compared with four AmB lipid formulations recently presented with remarkable temperature stability with about 80% after 30 to 60 days at 30 °C and 75% at 43 °C in drug content (34). Besides, AmB-PLGA-NS stored for 60-days at 30 °C behave similarly to fresh preparations as observed by the determination of the *in vitro* activity on *L. infantum* intracellular amastigotes. All these data allow us to affirm that the AmB-PLGA-NS are a sub-tropically stable formulation.

The effectiveness of the AmB-PLGA-NS was assessed in a VL susceptible murine model. The single-dose i.v. administration of AmBisome® resulted in 95.9%  $\pm$  1.1% to 99.0%  $\pm$  0.5% inhibition of spleen and liver parasites, respectively, consistent with literature reports (35, 36). When given in a single dose or 3-daily doses AmB-PLGA-NS led to a statistically significant reduction of splenic and liver parasites, corresponding to approximately 2-log<sub>10</sub> decrease, as compared to the vehicle control. Our data clearly demonstrate the advantageous efficacy of a single-dose of the AmB-PLGA-NS in reducing splenic parasites when compared to AmBisome® ( $P < 0.05$ ). This new DDS intravenously administered can be a promising approach for a structured VL treatment, preventing uncontrolled drug self-administration (e.g. oral route) as well as the emergence of AmB resistant strains.

In view of our *in vivo* results on VL murine model, we were interested in understanding the bio-distribution pattern of AmB when given as Fungizone®, AmBisome® and PLGA-NS by i.v. to infected animals. Both PLGA-NS (~ 200 nm) and AmBisome® (~ 100 nm) are particulate systems recognized by the mononuclear phagocyte system (MPS) (primarily liver, spleen and, to a lesser extent, lungs), while Fungizone®, a colloidal micellar system with about 1  $\mu$ m size, is able to avoid the effect of the MPS (37). In fact, Fungizone® displayed a more homogenous distribution on the tissues, with an evident retention in the kidney, which may be correlated with its well-known nephrotoxicity (38, 39). Interestingly, the concentration of AmB in tissues 2 h following i.v. administration of PLGA-NS and AmBisome® reveals some similarities. In both cases, most of the drug is found in major MPS-riched tissues, liver and spleen. Given the bio-distribution of PLGA-NS and AmBisome® among the splenic and hepatic tissues, these findings support the higher effectiveness of PLGA-NS observed in the splenic parasites reduction in the VL murine model.

The safety of the VL treatment is as fundamental as its effectiveness. By assessing the oxidative stress, a marker of drug-induced organ toxicity (40), it is possible to ascertain tissue toxicity elicited by the administration of the AmB treatments (25). Here we have evaluated the effects of all the VL treatments on the liver and spleen by quantifying several oxidative stress indicators. Given that the developed AmB-PLGA-NS exhibited similar oxidative stress levels when compared to AmBisome® and the untreated group it can be considered that identical drug-induced toxicity levels were caused in the liver or spleen. Nevertheless, extensive *in vivo* studies consisting of the assessment of nephrotoxicity and hepatotoxicity respectively of the new AmB-PLGA-NS will be addressed in the near future.

The profound impairment of the immune system of the infected host in VL is a major cause for incomplete efficacy of the anti-leishmanial chemotherapy, as the treatment success depends

INSTITUTO  
DE INVESTIGAÇÃO  
E INOVAÇÃO  
EM SAÚDE  
UNIVERSIDADE  
DO PORTO

Rua Alfredo Allen, 208  
4200-135 Porto  
Portugal  
+351 220 408 800  
info@i3s.up.pt  
[www.i3s.up.pt](http://www.i3s.up.pt)

on the combined effect of the drug itself and the immune status of the host (41, 42). Our results suggest that AmB-PLGA-NS improve the inherent immune-modulatory efficacy of AmB, most probably by directing towards a Th1 immune response, which is essential for a successful VL treatment. Th1 cells secreting large amounts of IFN- $\gamma$  will enhance cellular immunity by cytotoxic T lymphocytes and macrophages (43). It has been described the requirement of continuous presence of IL-12 for sustaining Th1 immunity, providing protective cell-mediated immune response towards murine *L. major* infection (44). Indeed, our data show a substantial reduction in splenic parasite burden and high levels of IL-12 and IFN- $\gamma$ , which verify these findings. Similarly, a high level of NO production in the AmB-PLGA-NS treated mice suggests the induction of NO-mediated macrophage effector mechanisms towards the control of parasite proliferation (45, 46). Moreover, IL-10 is considered to be the predominant immunosuppressive cytokine leading to susceptibility (47, 48). We detect a downregulation of IL-10 production either by lymphocytes or from other cellular origin. In this study, our results emphasize the importance of effective immune stimulation combined with anti-leishmanial activity for VL treatment. In the same way, it was described by others that AmB entrapped in stearylamine cationic liposomes was more effective in killing *L. donovani* and in retaining the immunomodulatory effect of free AmB on CD4<sup>+</sup> and CD8<sup>+</sup>-T cells for IFN- $\gamma$  production than AmBisome® (48). The AmB-PLGA-NS was able to preserve and develop the immunomodulatory effect already described for AmB (49), while AmBisome® did not, possibly due to different uptake mechanism and intracellular tracking of these two DDSs which may lead to different outcomes in the macrophage modulation and consequently T cells function.

As a final point the efficacy of AmB-PLGA-NS was correlated to the CD8<sup>+</sup>-T cells function. Currently, it is known that CD8<sup>+</sup>-T cells play an important role in the mechanisms for the cure and the resistance to *Leishmania* infection, either by the production of IFN- $\gamma$  and activation of macrophages, or by the direct killing of parasitized macrophages, or a combination of both effects (27, 28, 49). Therefore, targeting CD8<sup>+</sup>-T cells responses may have great therapeutic potential against VL.

Here we have demonstrated that the incorporation of AmB in PLGA-NS is able to reduce experimental VL when CD8<sup>+</sup>-T cells are present. Although nanoparticles are considered an efficient tool for inducing potent immune responses and several vaccine applications have been described (50), to the best of our knowledge, we describe here for the first time the crucial role of CD8<sup>+</sup>-T cells in the *in vivo* efficacy of a nano-therapy approach against intracellular *Leishmania* protozoan. Based on the present results, the developed AmB-PLGA-NS can be a promising approach for VL treatment, especially in tropical and subtropical developing countries where an affordable and effective approach is urgently needed.

## FUNDING

This work was supported by Fundo Europeu de Desenvolvimento Regional (FEDER) funds through the Operational Competitiveness Program-COMPETE and by national funds through Fundação para a Ciência e a Tecnologia under projects FCOMP-01-0124-FEDER-015718 (PTDC/SAU-ENB/113151/2009) and Fundação Calouste Gulbenkian under project P-105348/2009. D.B. was supported by FCOMP-01-0124-FEDER-015718 (PTDC/SAU-ENB/113151/2009) project. S.A.C.L., J.C. T.B. and R.D-O. were supported by SFRH/BPD/37880/2007, SFRH/BD/48626/2008, SFRH/BD/65387/2009 and IF/01147/2013, respectively. R.S. was supported by Programa Ciência, financed by Programa Operacional



Potencial Humano—Quadro de Referência Estratégica Nacional-Tipologia 4.2-Promoção do Emprego Científico, co-funded by Fundo Social Europeu and national funding from the Ministry of Science, Technology and Higher Education.

## COMPETING INTERESTS

There are no competing interests to report.

## REFERENCES

1. J. Torrado, R. Espada, M. Ballesteros, S. Torrado-Santiago **Amphotericin B formulations and drug targeting** J Pharm Sci, 7 (2008), pp. 2405-2425.
2. A. Lemke, A. Kiderlen, O. Kayser **Amphotericin B** Appl Microbiol Biotechnol, 68 (2005), pp. 151-162.
3. S. Sundar, H. Mehta, A. Suresh, S. Singh, M. Rai, H. Murray **AmB treatment for Indian visceral leishmaniasis: conventional versus lipid formulations** Clin Infect Dis, 38 (2004), pp. 377-383.
4. J. Brajtburg, J. Bolard **Carrier effects on biological activity of AmB** Clin Microbiol Rev, 9 (1996), pp. 512-531.
5. F. Meheus, M. Balasegaram, P. Olliaro **Cost-effectiveness analysis of combination therapies for visceral leishmaniasis in the Indian subcontinent** PLoS Negl Trop Dis, 4 (2010), p. 818.
6. L. Guo **Amphotericin B, colloidal dispersion: an improved antifungal therapy** Adv Drug Deliv Rev, 47 (2001), pp. 149-163.
7. J. Adler-Moore, R. Proffitt **Amphotericin B lipid preparations: what are the differences** Clin Microbiol Infect, 14 (2008), pp. 25-36.
8. S. Sundar, J. Chakravarty, D. Agarwal, M. Rai, H. Murray **Single-dose liposomal amphotericin B for visceral leishmaniasis in India** N Engl J Med, 362 (2010), pp. 504-512.
9. G. Boswell, D. Buell, I. Bekersky **AmBisome (liposomal amphotericin B): a comparative review** J Clin Pharmacol, 38 (1998), pp. 538-592.
10. T. Walsh, R. Finberg, C. Arndt, J. Hiemenz, C. Schwartz, D. Bodensteiner, *et al.* **Liposomal amphotericin B for empirical therapy in patients with persistent fever and neutropenia** N Engl J Med, 340 (1999), pp. 764-771.
11. I. Bekersky, R. Fielding, D. Buell, I. Lawrence **Lipid-based amphotericin B formulations: from animals to man** Pharm Sci Technol Today, 2 (1999), pp. 230-236.
12. I. Bekersky, R. Fielding, D. Dressler, J. Lee, D. Buell, T. Walsh **Pharmacokinetics, excretion, and mass balance of liposomal amphotericin B (AmBisome) and**

INSTITUTO  
DE INVESTIGAÇÃO  
E INOVAÇÃO  
EM SAÚDE  
UNIVERSIDADE  
DO PORTO

Rua Alfredo Allen, 208  
4200-135 Porto  
Portugal  
+351 220 408 800  
info@i3s.up.pt  
[www.i3s.up.pt](http://www.i3s.up.pt)

**amphotericin B deoxycholate in humans** *Antimicrob Agents Chemother*, 46 (2002), pp. 828-834.

13. A.J. Atkinson, J. Bennett **Amphotericin B pharmacokinetics in humans** *Antimicrob Agents Chemother*, 13 (1978), pp. 271-276.

14. S. Jung, D. Lim, S. Jung, J. Lee, K.-S. Jeong, H. Seong, *et al.* **Amphotericin B-entrapping lipid nanoparticles and their *in vitro* and *in vivo* characteristics** *Eur J Pharm Sci*, 37 (2009), pp. 313-320.

15. H. Van de Ven, C. Paulussen, P. Feijens, A. Matheussen, P. Rombaut, P. Kayaert, *et al.* **PLGA nanoparticles and nanosuspensions with amphotericin B: potent *in vitro* and *in vivo* alternatives to Fungizone and Am Bisome** *J Control Release*, 161 (2012), pp. 795-803.

16. J. Italia, A. Sharp, K. Carter, P. Warn, M. Kumar **Peroral amphotericin B polymer nanoparticles lead to comparable or superior *in vivo* antifungal activity to that of intravenous Ambisome® or Fungizone™** *PLoS One*, 6 (2011), p. e25744.

17. Z. Yang, Y. Tan, M. Chen, L. Dian, Z. Shan, X. Peng, *et al.* **Development of amphotericin B-loaded cubosomes through the solemls technology for enhancing the oral bioavailability** *AAPS PharmSciTech*, 13 (2012), pp. 1483-1491.

18. J. Jain, M. Jatana, A. Chakrabarti, N. Kumar **Amphotericin-B-loaded polymersomes formulation (PAMBO) based on (PEG)3-PLA copolymers: an *in vivo* evaluation in a murine model** *Mol Pharm*, 8 (2011), pp. 204-212.

19. V. Prajapati, K. Awasthi, S. Gautam, T. Yadav, M. Rai, O. Srivastava, *et al.* **Targeted killing of *Leishmania donovani* *in vivo* and *in vitro* with amphotericin B attached to functionalized carbon nanotubes** *J Antimicrob Chemother*, 66 (2011), pp. 874-879.

20. S. Vyas, S. Gupta **Optimizing efficacy of amphotericin B through nanomodification** *Int J Nanomedicine*, 1 (2006), pp. 417-432.

21. M. Chavanpatil, A. Khair, J. Panyam **Nanoparticles for cellular drug delivery: mechanisms and factors influencing delivery** *J Nanosci Nanotechnol*, 6 (2006), pp. 2651-2663.

22. H. Fessi, F. Puisieux, J. Devissaguet, N. Ammoury, S. Benita **Nanocapsule formation by interfacial polymer deposition following solvent displacement** *Int J Pharm*, 55 (1989), pp. R1-R4.

23. R. Espada, J. Josa, S. Valdespina, M. Dea, M. Ballesteros, J. Alunda, *et al.* **HPLC assay for determination of amphotericin B in biological samples** *Biomed Chromatogr*, 22 (2008), pp. 402-407.

24. A. Ding, C. Nathan, D. Stuehr **Release of reactive nitrogen intermediates and reactive oxygen intermediates from mouse peritoneal macrophages. Comparison of activating cytokines and evidence for independent production** *J Immunol*, 141 (1988), pp. 2407-2412.

25. N. Paniker, S. Srivastava, E. Beutler **Glutathione metabolism of the red cells. Effect of glutathione reductase deficiency on the stimulation of hexose monophosphate shunt under oxidative stress** *Biochim Biophys Acta*, 215 (1970), pp. 456-460.
26. T. Bousoffara, H. Louzir, A. Ben Salah, K. Dellagi **Analysis of granzyme B activity as a surrogate marker of *Leishmania*-specific cell-mediated cytotoxicity in zoonotic cutaneous leishmaniasis** *J Infect Dis*, 189 (2004), pp. 1265-1273.
27. Z. Wang, S. Reiner, S. Zheng, D. Dalton, R. Locksley **CD4<sup>+</sup> effector cells default to the Th2 pathway in interferon gamma-deficient mice infected with *Leishmania major*** *J Exp Med*, 179 (1994), pp. 1367-1371.
28. Y. Belkaid, E. Von Stebut, S. Mendez, R. Lira, E. Caler, S. Bertholet, *et al.* **CD8<sup>+</sup> T cells are required for primary immunity in C57BL/6 mice following low-dose, intradermal challenge with *Leishmania major*** *J Immunol*, 168 (2002), pp. 3992-4000.
29. S.M. Moghimi, A.C. Hunter, J.C. Murray **Long-circulating and target specific nanoparticles: theory to practice** *Pharmacol Rev*, 53 (2001), pp. 283-318.
30. R.A. Jain **The manufacturing techniques of various drug loaded biodegradable poly(lactide-co-glycolide) devices** *Biomaterials*, 21 (2000), pp. 2475-2490.
31. J. Barichello, M. Morishita, K. Takayama, T. Nagai **Encapsulation of hydrophilic and lipophilic drugs in PLGA nanoparticles by the nanoprecipitation method** *Drug Dev Ind Pharm*, 25 (1999), pp. 471-476.
32. S. Vrignaud, J. Benoit, P. Saulnier **Strategies for the nanoencapsulation of hydrophilic molecules in polymer-based nanoparticles** *Biomaterials*, 33 (2011), pp. 8593-8604.
33. D. Quintanar-Guerrero, A. Ganem-Quintanar, E. Allémann, H. Fessi, E. Doelker **Influence of the stabilizer coating layer on the purification and freeze-drying of poly(D, L-lactic acid) nanoparticles prepared by an emulsion-diffusion technique** *J Microencapsul*, 15 (1998), pp. 107-119.
34. E. Wasan, P. Gershkovich, J. Zhao, X. Zhu, K. Werbovetz, R. Tidwell, *et al.* **A novel tropically stable oral amphotericin B formulation (iCo-010) exhibits efficacy against visceral leishmaniasis in a murine model** *PLoS Negl Trop Dis*, 4 (2010), p. e913.
35. V.K. Prajapati, K. Awasthi, T.P. Yadav, M. Rai, O.N. Srivastava, S. Sundar **An oral formulation of amphotericin B attached to functionalized carbon nanotubes is an effective treatment for experimental visceral leishmaniasis** *J Infect Dis*, 205 (2012), pp. 333-336.
36. J. Gangneux, A. Sulahian, Y. Garin, R. Farinotti, F. Derouin **Therapy of visceral leishmaniasis due to *Leishmania infantum*: experimental assessment of efficacy of Am Bisome** *Antimicrob Agents Chemother*, 40 (1996), pp. 1214-1218.
37. H. Fukui, T. Koike, T. Nakagawa, A. Saheki, S. Sonoke, Y. Tomii, *et al.* **Comparison of LNS-AmB, a novel low-dose formulation of amphotericin B with lipid nano-sphere (LNS), with commercial lipid-based formulations** *Int J Pharm*, 267 (2003), pp. 101-112.

38. R. Fielding, A. Singer, L. Wang, S. Babbar, L. Guo **Relationship of pharmacokinetics and drug distribution in tissue to increased safety of amphotericin B colloidal dispersion in dogs** *Antimicrob Agents Chemother*, 36 (1992), pp. 299-307.
39. I. Bekersky, G. Boswell, R. Hiles, R. Fielding, D. Buell, T. Walsh **Safety, toxicokinetics and tissue distribution of long-term intravenous liposomal amphotericin B (AmBisome): a 91-day study in rats** *Pharm Res*, 17 (2000), pp. 1494-1502.
40. C.V. Pereira, S. Nadanaciva, P.J. Oliveira, Y. Will **The contribution of oxidative stress to drug-induced organ toxicity and its detection *in vitro* and *in vivo*** *Expert Opin Drug Metab Toxicol*, 8 (2012), pp. 219-237.
41. P. Sharma, N. Singh, R. Garg, W. Haq, A. Dube **Efficacy of human  $\alpha$ -casein fragment (54–59) and its synthetic analogue compound 89/215 against *Leishmania donovani* in hamsters** *Peptides*, 25 (2004), pp. 1873-1881.
42. E. Carvalho, R. Teixeira, W.J. Johnson **Cell-mediated immunity in American visceral leishmaniasis: reversible immunosuppression during acute infection** *Infect Immun*, 33 (1981), pp. 498-500.
43. S. Reiner, R. Locksley **The regulation of immunity to *Leishmania major*** *Annu Rev Immunol*, 13 (1995), pp. 151-177.
44. T. Joshi, S. Rodriguez, V. Perovic, I. Cockburn **Stager pp. B7-H1 blockade increases survival of dysfunctional CD8(+) T cells and confers protection against *Leishmania donovani* infections** *PLoS Pathog*, 5 (2009), p. e1000431.
45. R. Polley, S. Stager, S. Prickett, A. Maroof, S. Zubairi, D. Smith, *et al.* **Adoptive immunotherapy against experimental visceral leishmaniasis with CD8 + T cells requires the presence of cognate antigen** *Infect Immun*, 74 (2006), pp. 773-776.
46. J. Moon, B. Huang, D. Irvine **Engineering nano- and microparticles to tune immunity** *Adv Mater*, 24 (2012), pp. 3724-3746.
47. B.M. Owens, L. Beattie, J.W. Moore, N. Brown, J.L. Mann **IL-10-producing Th1 cells and disease progression are regulated by distinct CD11c(+) cell populations during visceral leishmaniasis** *PLoS Pathog*, 8 (2012), p. e1002827.
48. A. Banerjee, M. De, N. Ali **Complete cure of experimental visceral leishmaniasis with amphotericin B in stearylamine-bearing cationic liposomes involves down-regulation of IL-10 and favorable T cell responses** *J Immunol*, 181 (2008), pp. 1386-1398.
49. H. Murray, E. Brooks, J. DeVecchio, F. Heinzl **Immunoenhancement combined with amphotericin B as treatment for experimental visceral leishmaniasis** *Antimicrob Agents Chemother*, 47 (2003), pp. 2513-2517.
50. P. Tsagozis, E. Karagouni, E. Dotsika **CD8(+) T cells with parasite-specific cytotoxic activity and aTc1 profile of cytokine and chemokine secretion develop in experimental visceral leishmaniasis** *Parasite Immunol*, 25 (2003), pp. 569-579.

## TABLES & FIGURES

**Table 1.** Physicochemical characterization of the nanospheres

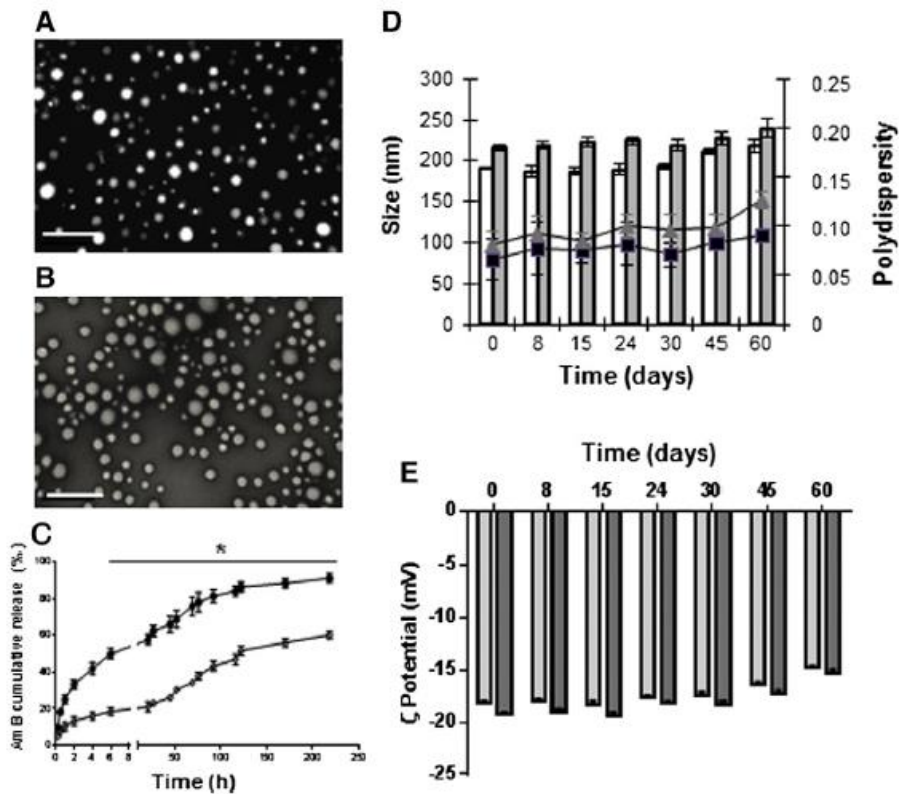
Nanospheres	Size (nm)	PDI	$\xi$ -potential (mV)	Encapsulation efficiency (%)
PLGA-NS	187.3 $\pm$ 1.3	0.06 $\pm$ 0.02	-18.2 $\pm$ 0.8	NA
AmB-PLGA-NS	221.5 $\pm$ 6.6*	0.09 $\pm$ 0.03	-18.9 $\pm$ 0.9	65.4 $\pm$ 4.7

Data are expressed as the mean  $\pm$  SEM (n = 6). NA, not applicable; \* $P < 0.05$ , statistically significant when compared to empty nanospheres.

**Table 2.** Tissue distribution of AmB 2 h following i.v. administration of PLGA-NS, Fungizone® and AmBisome®.

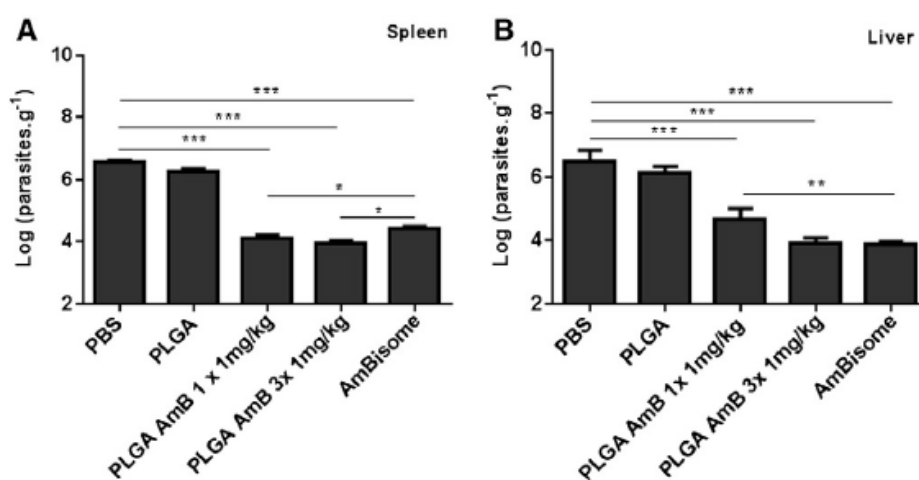
Tissue	Treatment group		
	Fungizone®	AmBisome®	AmB-PLGA-NS
Liver	541 $\pm$ 65	5148 $\pm$ 426	2456 $\pm$ 288
Kidney	895 $\pm$ 81	539 $\pm$ 56	184 $\pm$ 26
Spleen	286 $\pm$ 27	2934 $\pm$ 286	4225 $\pm$ 354
Lung	45 $\pm$ 8	215 $\pm$ 18	95 $\pm$ 12
Heart	32 $\pm$ 4	248 $\pm$ 22	42 $\pm$ 3

ng/g, mean  $\pm$  SEM, n = 6.

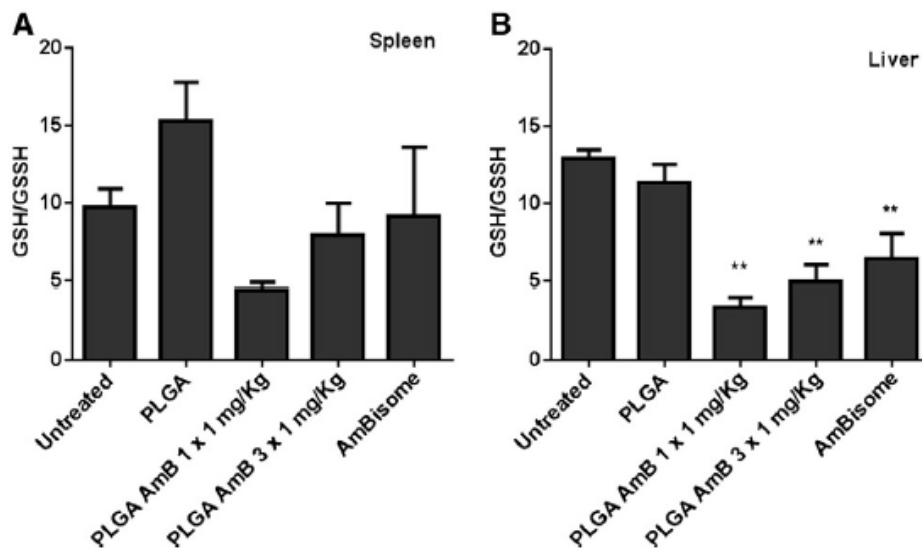


**Figure 1.** Characterization of the AmB-PLGA nanospheres. Morphology of unloaded (**A**) and AmB-loaded (**B**) PLGA-NS; scale bar is 500 nm. (**C**) AmB *in vitro* release kinetics from PLGA-NS at pH 5.5 (●) and pH 7.4 (◇); means ± SDs (n = 5). (**D**) Storage stability for unloaded (white bars; squares) and AmB-loaded (dark bars; triangles) PLGA-NS at 4 °C for 2-months according to size (bars) and PDI (lines) and (**E**) ζ-potential.

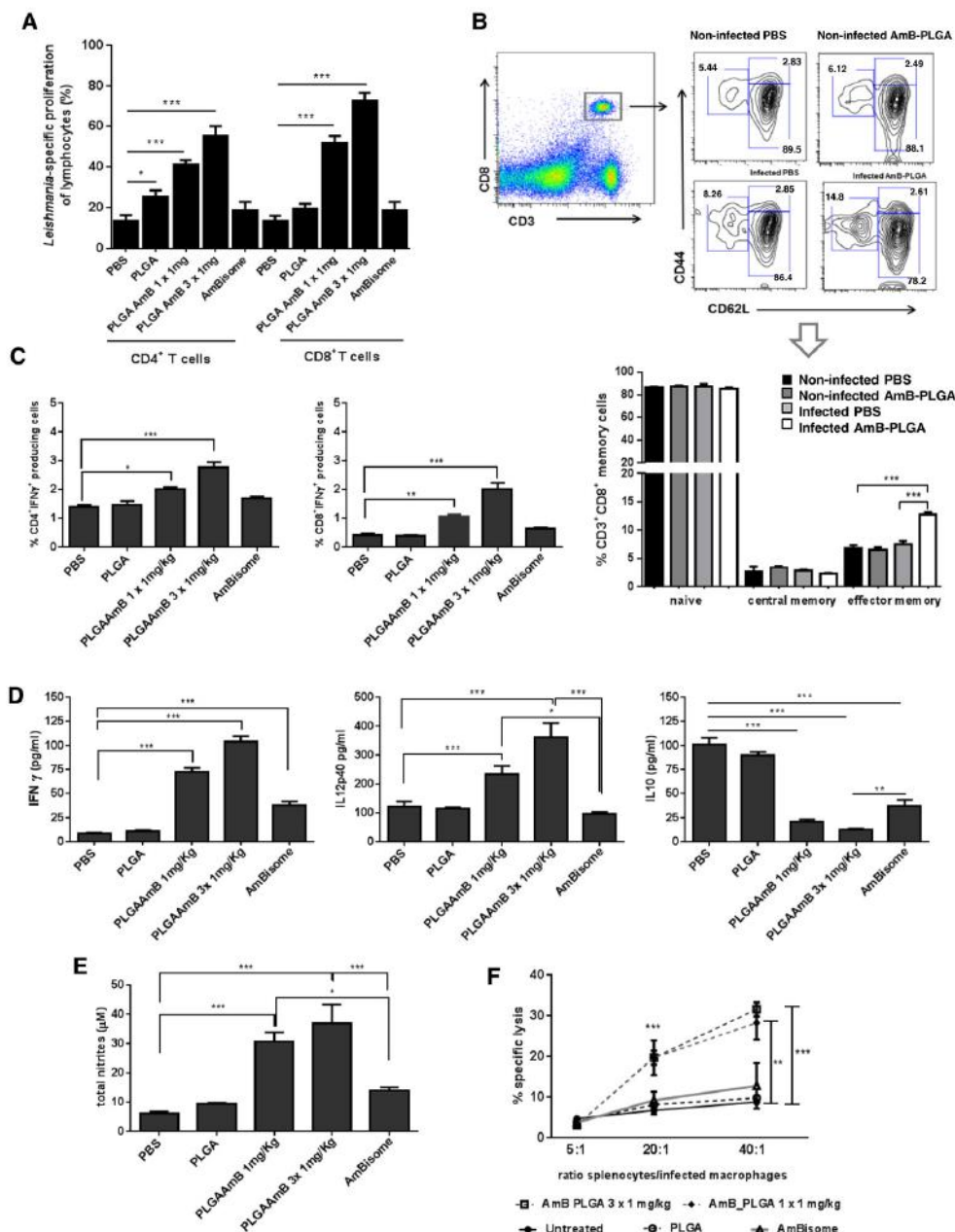




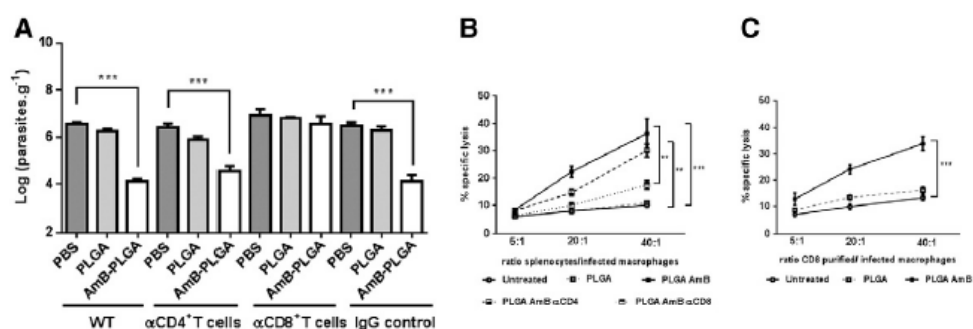
**Figure 2.** *In vivo* efficacy of AmB-PLGA nanospheres in *L. infantum*-infected mice. 3-days after the last administration, parasite burden was evaluated by limiting dilution assay in the spleen (A) and in the liver (B). Data represent the mean  $\pm$  SD of a representative experiment from two carried out independently, with six mice per experimental group in each experiment \* $P < 0.05$ , \*\* $P < 0.01$  and \*\*\* $P < 0.001$  in comparison with untreated group.



**Figure 3.** Measurement of the ratio of reduced glutathione to oxidized glutathione. **(A)** Liver and **(B)** spleen of *Leishmania*-infected mice untreated or treated. Values are given as mean  $\pm$  SEM ( $n = 4$ ). The comparison between untreated infected group and the different treatment groups was made with the one-way analysis of variance (ANOVA) with Dunnett's multiple comparison test.

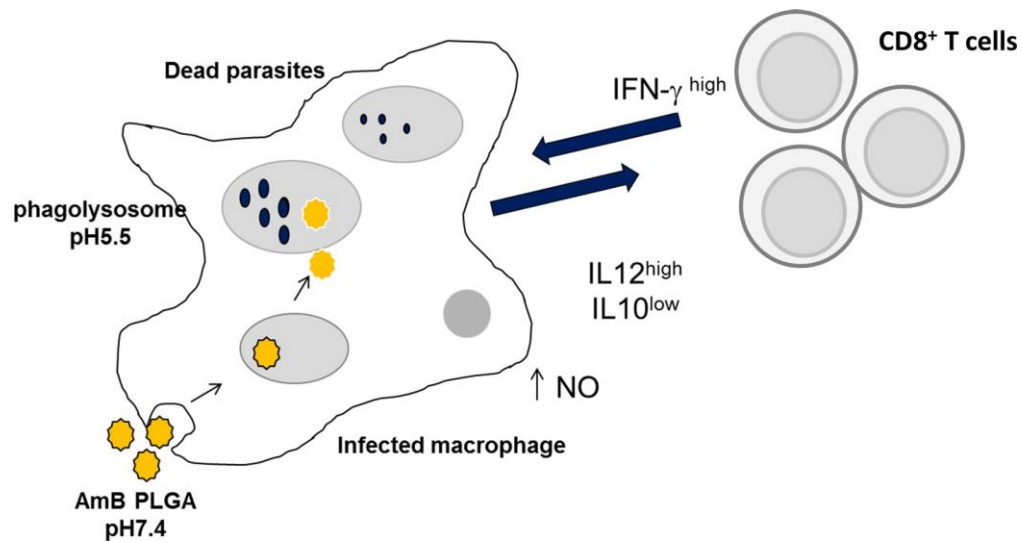


**Figure 4.** *In vivo* mechanism of AmB-PLGA nanospheres in *L. infantum*-infected mice. **(A)** *In vitro* proliferation of splenic cells of differently treated mice. **(B)** Phenotype of CD8<sup>+</sup> memory T cells. **(C)** Intracellular and secreted IFN- $\gamma$ , IL-12p40 and IL-10 production of total CD4<sup>+</sup>- and CD8<sup>+</sup>-T cells from all experimental groups. **(E)** NO production. **(F)** AmB-PLGA-NS treatment causes a *Leishmania*-specific cytotoxic response. Data represent the mean  $\pm$  SD of a representative experiment from two carried out independently, with six mice per experimental group in each experiment \* $P < 0.05$ , \*\* $P < 0.01$  and \*\*\* $P < 0.001$  in comparison with untreated group.



**Figure 5.** CD8<sup>+</sup>-T cells are crucial for the in vivo efficacy of AmB-PLGA nanospheres in *L. infantum*-infected mice. (A) Parasite load in PBS, PLGA-NS or AmB-PLGA-NS treated mice depleted of CD4<sup>+</sup> and CD8<sup>+</sup>-T cells prior treatment. Untreated and (PBS) treated mice with IgG were used as controls. (B, C) AmB-PLGA-NS treatment causes a *Leishmania*-specific cytotoxic response dependent on CD8<sup>+</sup>-T cells. Data represent the mean ± SD of a representative experiment from two carried out independently, with four mice per experimental group in each experiment \*P < 0.05, \*\*P < 0.01 and \*\*\*P < 0.001 in comparison with untreated group.

## GRAPHICAL ABSTRACT



Proposed mechanism of action of AmB-PLGA nanospheres on *Leishmania*-infected macrophages and interaction with CD8<sup>+</sup> T cells.